Characteristic analysis of fractional-order simplest chaotic circuit based on Adomian decomposition method

Haiying Hu[1], Yinghong Cao[2], Huizhen Yan[3]

{cncaoyinghong@dlpu.edu.cn}

School of Information Science and Engineering, Dalian polytechnic University, Dalian, 116034, China

Abstract: In this paper, a fractional order chaotic system is reconstructed in the simplest memristive chaotic circuit. The solution of this system is obtained through ADM. Phase diagrams, LEs, bifurcation diagrams and complexity are used in the dynamics study of this fractional chaotic system. At the same time, the stability of the chaotic circuit is concluded and its stability region is given. Meanwhile, the digital circuit of the system was designed and verified on the DSP board. Research results indicate that the ADM algorithm can accurately analyze and calculate effective numerical solutions of fractional-order chaotic systems. According to dynamic analysis, we can get that the system has complex dynamic behavior. This article provides a new direction for the study of the simplest fractional-order memristive chaotic circuits, and provides guidance for the application of proposed systems in the actual field.

Key words: ADM decomposition algorithm; fractional-order memristive chaotic circuit; dynamical characteristic; DSP implementation

1. Introduction

In 1971, Professor Cai reported the memristor for the first time and analyzed the relevant content of the memristor [1], and elaborated on the physical characteristics, basic principles and applications of memristive in 1976 [2]. For a long time, since the actual components that meet the characteristics of the memristive have not been discovered, the research on the memristive

EAI GreeNets 2021, June 06-07, Dalian, People's Republic of China

DOI 10.4108/eai.6-6-2021.2307855

has not yet attracted scholars' attention.. It was not until 2008 that HP Labs reported the hardware implementation of the memristor for the first time [3], which made the research of memristive aroused widespread concern all over the world.

Memristive usually includes two types of typical nonlinear elements: charge-controlled memristive and magnetron memristive. Because memristive have memory characteristics, and non-linear circuits based on memristor elements are more likely to produce chaotic signals. Scholars have been focusing on the design and implementation of memristive chaotic circuits and have made great progress [4-11]. Fernando et al. analyzed the dynamical behaviors of one kind of memristor oscillators [4]. A simplest chaotic fractional memristor was proposed by Lin et al. [5]. Bao et al. constructed some new circuits based on the smooth memristive model and found that their dynamic behavior is closely related to the initial conditions [6]. The six synchronization algorithms for chaotic systems based on memristor is presented in Ref. [7]. Ye et al. [8, 9] reached the complexity of the hybrid memristive chaotic circuit and analyzed a novel 5-D hyperchaotic memristive system. Most of the existing researches on memristive chaotic circuits are aimed at chaotic systems of integer order.

However, many references indicate that fractional-order chaotic systems have better performance chaotic sequences, higher complexity and richer dynamics, which are more suitable for the field of secure communication [12-19]. Therefore, the relevant research on the dynamics of fractional-order chaotic circuits with memristor is curious. It is very meaningful to research the dynamics of fractional-order chaotic circuits based on a simplest memristive chaotic circuit.

For discretizing fractional-order chaotic systems, the existing references mostly use frequency domain approximation methods[20], predictor-corrector method, and Adomian decomposition method (ADM) [21]. Among them, ADM has the advantages of better accuracy of calculation results and faster calculation speed, and is more suitable for solving fractional differential equations than other decomposition methods [24, 25]. Therefore, we choose ADM algorithm to solve the chaotic system.

In this paper, a fractional-order chaotic equation is constructed based on the circuit containing the simplest memristor and its dynamic behavior is analyzed. Its organizational structure: In Section 2, the memristor is introduced and the simplest memristive circuit model is proposed. In Section 3, the ADM algorithm discretizes the simplest fractional order chaotic circuit system equation and obtains its numerical solution. In Section 4, the dynamics of the system are studied. Design and implement the digital circuit of the system on the DSP platform. Finally, some experimental conclusions are summarized.

2. Simplest Memristive Chaotic Circuit

2.1 Introduction to the memristive model

The memristor model is used to illustrate the connection between magnetic charge q and flux φ. The q and φ passing through the memristive can be represented by a curve $f(\varphi, q)=0$ in the rectangular coordinate system. If the magnetic flux φ plays a dominant role, then the memristor is called a magnetron memristor, and $W(\varphi)=dq(\varphi)d\varphi$, here $W(\varphi)$ is called its meminductor value, and the volt-ampere characteristic between the current flowing through the element and the voltage at both ends is $i(t)=w(\varphi)u(t)$; If the amount of charge in the memristor plays a leading role, then the memristor is a charge-controlled memristor, and $M(q)=d\varphi(q)/dq$, here $M(q)$ is called its memristive value, the volt-ampere characteristic between the current flowing pass the memristive and the voltage across it is $u(t)= M(q)i(t)$. Memristive usually has basic criteria such as passivity, closure, existence, uniqueness, and complexity. At present, the real realization of the memristor is still at the experimental level, so the research on the memristor at this stage is mainly aimed at its equivalent circuit model or mathematical model.

2.2 The memristive circuit model□

Figure 1 plotted the simplest memristive circuit model.

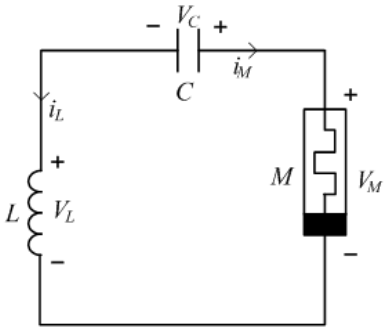

Fig. 1 Simplest memristive circuit

where M, V_M, V_L, V_C, i_M and i_L is the state variables. The memristor model can be expressed as

$$\begin{cases} V_M = \beta(z^2-1)i_M \\ \dot{z} = i_M - \alpha z - z i_M \end{cases} \tag{1}$$

The circuit model can be obtained by equations (2).

$$\begin{cases} \mathrm{C}\dfrac{dV_C(t)}{dt} = i_L(t) \\ L\dfrac{di_L(t)}{dt} = -(V_C(t) + \beta(z^2(t)-1)i_L(t)) \\ \dfrac{dz(t)}{dt} = i_L(t) - \alpha z(t) + i_L(t)z(t) \end{cases} \tag{2}$$

Let $1/C=c$, $1/L=d$, $V_C(t)=x$, $i_L(t)=y$, $z(t)=z$, the normalization operation of Eq. (2) is:

$$\begin{cases} \dot{x} = cy \\ \dot{y} = -d(x + \beta z^2 y - \beta y), \\ \dot{z} = -y(-\alpha + y)z \end{cases} \tag{3}$$

here the system parameters are c, α, β, d, set α=0.6, c=1, β=1.5, d=1/3, and the initial values are [0.1, 0, 0]. The Lyapunov exponent can be calculated as follows: L_1=0.045, L_2=0, L_3=-0.603. A Lyapunov exponent is greater than 0 proves that the system is chaotic with this parameter.

Combining the definition of Caputo's fractional differential with the Eq. (3), a fractional system equation is reconstructed. The expression equation is as follows

$$\begin{cases} {}^*D_{t_0}^q x = cy \\ {}^*D_{t_0}^q y = -d(x + \beta(z^2 - 1)y), \\ {}^*D_{t_0}^q z = -y - \alpha z + yz \end{cases} \tag{4}$$

Among them t_0 is the initial value, ${}^*D_{t_0}^q$ is the Caputo operator, q is the order ($0<q\leq 1$).

3. The solution of chaotic system

3.1 ADM decomposition algorithm

A fractional differential equation ${}^*D_{t_0}^q(t)=f(x(t))$, $x(t)=[x_1(t), x_2(t), x_3(t), \ldots, x_n(t)]^T$ is a function variable, and ${}^*D_{t_0}^q$ denotes q-order Caputo differential operator, then the system can expressed by

$$\begin{cases} {}^{*}D_{t_0}^{q}x(t) = Nx(t) + Lx(t) + g(t) \\ x^{(k)}(t_0^{+}) = b_k, k = 0,1,...,m-1 \\ g(t) = [g_1(t), g_2(t), \text{K}, g_n(t)]^T \end{cases}, \tag{5}$$

here, N represents the nonlinear term of the differential equation. L is the linear part of the Eq. (1), $g(t)$ is constant of the autonomous system, and b_k is given initial value. After performing operations of Eq. (4), we can get

$$x = J_{t_0}^{q}Nx + J_{t_0}^{q}Lx + J_{t_0}^{q}g + \sum_{k=0}^{m-1} b_k \frac{(t-t_0)^k}{k!} , \tag{6}$$

here, $J_{t_0}^{q}$ is the R-L fractional integral operator of order q (q⩾0). The basic features of this operator are

$$J_{t_0}^{q}(t-t_0)^{\gamma} = \frac{\Gamma(l+1)}{\Gamma(l+1+q)}(t-t_0)^{l+q}, \tag{7}$$

$$J_{t_0}^{q}C = \frac{C}{\Gamma(q+1)}(t-t_0)^{q}, \tag{8}$$

$$J_{t_0}^{q}J_{t_0}^{r}x(t) = J_{t_0}^{q+r}x(t), \tag{9}$$

where C is a constant, l≥-1, r≥0, t∈[t_0,t_1],. As a nonlinear term, N needs to be further decomposed. The decomposition rules are as follows

$$\begin{cases} A_j^i = \frac{1}{i!}[\frac{d^i}{d\lambda^i}N(v_j^i(\lambda))]_{\lambda=0} \\ v_j^i(\lambda) = \sum_{k=0}^{i}(\lambda)^k x_j^k \end{cases}, \tag{10}$$

Among them j=1, 2, 3, …, n, i=0, 1, 2, 3, … , ∞. The nonlinear term is

$$Nx = \sum_{i=0}^{\infty} A^i(x^0, x^1, ..., x^i). \tag{11}$$

From equation (11), the solution of equation (5) is

$$\begin{cases} x^0 = J_{t_0}^q g + \sum_{k=0}^{m-1} b_k \dfrac{(t-t_0)^k}{k!} \\ x^1 = J_{t_0}^q L x^0 + J_{t_0}^q A^0(x^0) \\ \cdots \\ x^i = J_{t_0}^q L x^{i\text{-}1} + J_{t_0}^q A^{i\text{-}1}(x^0, x^1, \ldots, x^{i\text{-}1}) \\ \cdots \end{cases} . \tag{12}$$

3.2 Solution of Fractional Memristive Chaotic System

The iterative algorithm of the chaotic system is:

$$\begin{cases} x_{m+1} = x_m + c y_m \dfrac{h^q}{\Gamma(q+1)} + cd(x_m - \beta y_m + \beta y_m z_m^2) \\ \quad \dfrac{h^{2q}}{\Gamma(2q+1)} + \ldots \\ y_{m+1} = y_m + c(x_m - \beta y_m + \beta y_m z_m^2) \dfrac{h^q}{\Gamma(q+1)} \\ \quad + (cdy_m - d^2 \beta x_m + \ldots) \dfrac{h^{2q}}{\Gamma(2q+1)} + \ldots \\ z_{m+1} = z_m + (y_m z_m - y_m - \alpha z_m) \dfrac{h^q}{\Gamma(q+1)} + (z_m b x_m \\ +\ldots) \quad \dfrac{h^{2q}}{\Gamma(2q+1)} + \ldots \end{cases} . \tag{13}$$

Here, the step size is set h. the iteration algorithm are

$$\begin{cases} C_{10} = x_m \\ C_{20} = y_m \\ C_{30} = z_m \end{cases} . \tag{14}$$

$$\begin{cases} C_{11} = cC_{20} \\ C_{21} = dC_{10} - d\beta C_{20} + d\beta C_{20}C_{30}^2 \\ C_{30} = -C_{20} - \alpha C_{30} + C_{20}C_{30} \end{cases}. \tag{15}$$

$$\begin{cases} C_{12} = cC_{21} \\ C_{22} = dC_{11} - d\beta C_{21} + d\beta(C_{21}C_{30}^2 + 2C_{20}C_{30}C_{31}) \\ C_{32} = -C_{21} - \alpha C_{31} + C_{21}C_{30} + C_{20}C_{31} \end{cases}. \tag{16}$$

$$\begin{cases} C_{13} = cC_{22} \\ C_{23} = dC_{12} - d\beta C_{22} + d\beta(C_{22}C_{30}^2 + 2C_{20}C_{30}C_{32}) \\ \quad + d\beta(2C_{21}C_{30}C_{21} + C_{20}C_{31}^2)\dfrac{\Gamma(2q+1)}{\Gamma^2(q+1)} \\ C_{33} = -C_{22} - \alpha C_{32} + C_{22}C_{30} + C_{20}C_{32} + C_{21}C_{31} \\ \quad \dfrac{\Gamma(2q+1)}{\Gamma^2(q+1)} \end{cases}. \tag{17}$$

$$\begin{cases} C_{14} = cC_{23} \\ C_{24} = dC_{13} - d\beta C_{23} + d\beta(C_{23}C_{30}^2 + 2C_{20}C_{30}C_{33} + \\ \quad (2C_{22}C_{30}C_{31} + 2C_{21}C_{30}C_{32} + 2C_{20}C_{31}C_{32}) \\ \quad \dfrac{\Gamma(3q+1)}{\Gamma(q+1)\Gamma(2q+1)} + C_{21}C_{31}^2\dfrac{\Gamma(3q+1)}{\Gamma^3(q+1)}) \\ C_{34} = -C_{23} - \alpha C_{33} + C_{23}C_{30} + C_{20}C_{33} + (C_{21}C_{32} \\ \quad + C_{22}C_{31})\dfrac{\Gamma(3q+1)}{\Gamma(q+1)\Gamma(2q+1)} \end{cases}. \tag{18}$$

$$
\begin{cases}
C_{15} = cC_{24} \\
C_{25} = dC_{14} - d\beta C_{24} + d\beta(C_{24}C_{30}^2 + 2C_{20}C_{30}C_{34} \\
\quad +(2C_{23}C_{30}C_{31} + 2C_{21}C_{30}C_{33} + 2C_{20}C_{31}C_{33}) \\
\quad \frac{\Gamma(4q+1)}{\Gamma(q+1)\Gamma(3q+1)} + (2C_{22}C_{30} + C_{20}C_{32}^2)\frac{\Gamma(4q+1)}{\Gamma^2(2q+1)} \cdot \\
\quad +(C_{22}C_{31}^2 + 2C_{21}C_{31}C_{32})\frac{\Gamma(4q+1)}{\Gamma(2q+1)\Gamma^2(q+1)}) \\
C_{35} = -C_{24} - \alpha C_{34} + C_{24}C_{30} + C_{20}C_{34} + (C_{23}C_{31} \\
\quad +C_{21}C_{33})\frac{\Gamma(4q+1)}{\Gamma(q+1)\Gamma(3q+1)} + C_{22}C_{32}\frac{\Gamma(4q+1)}{\Gamma^2(2q+1)}
\end{cases} \tag{19}
$$

3.3 Solution of the Lyapunov exponents spectra

Based on the QR decomposition and iterative formula, the algorithm of Lyapunov exponential spectrum calculation of chaotic system is designed. And QR decomposition is

$$
\begin{aligned}
& qr[J_h ... J_1] \\
& = qr[J_h J_{h-1} ... J_2 (J_1 Q_0)] \\
& = qr[J_h J_{h-1} ... J_3 (J_2 Q_1)][R_1] \\
& = qr[J_h J_{h-1} ... (J_i Q_{i-1})][R_{i-1} R_{i-2} ... R_2 R_1] . \\
& = ... \\
& = Q_h [R_h ... R_1] \\
& = Q_h R
\end{aligned} \tag{20}
$$

where QR decomposition process is represented by $qr[\cdot]$. Jacobian matrix is expressed by J, and h represents the number of iteration. Then we get the LE spectrum

$$
\lambda_k = \frac{1}{mh}\sum_{i=1}^{m} \ln\left|R_i(k,k)\right|, \tag{21}
$$

here k is the system dimension.

4. Analysis of dynamic characteristics of chaotic system and DSP realization

4.1 Stability analysis

Let $-b(x+\beta(z^2-1)y)=0$, $ay=0$, $y-\alpha z+yz=0$. Obviously, there is an equilibrium point, which is $x=y=z=0$. The Jacobian matrix is

$$J_{(P_0)}=\begin{bmatrix} 0 & a & 0 \\ -b & b\beta & 0 \\ 0 & 1 & -\alpha \end{bmatrix}. \tag{22}$$

In the equilibrium point, $(\lambda+\alpha)(\lambda^2-b\beta\lambda+ab)=0$ is the characteristic polynomial of the Eq. (22), and the characteristic root of the characteristic polynomial is

$$\begin{cases} \lambda_1=-\alpha \\ \lambda_2=(b\beta+j\sqrt{4ab-b^2\beta^2})/2 \\ \lambda_3=(b\beta-j\sqrt{4ab-b^2\beta^2})/2 \end{cases} \tag{23}$$

According to the chaotic system equilibrium point analysis theorem[16], the system stability can be analyzed in detail as follows.

Theorem 1: If all the characteristic roots of a chaotic system satisfy $|\arg(\mathrm{eig}(J))|=|\arg(\lambda_i)|>q\pi/2$ ($i=1, 2, 3, \ldots, n$), it indicates the system is gradually stable.

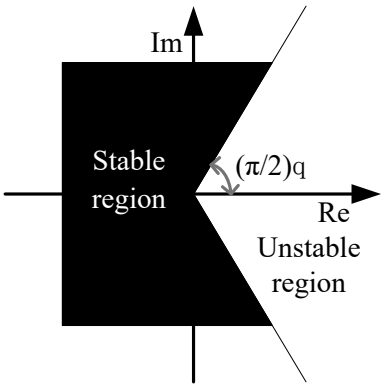

Fig.2 Unstable and stable regions in f chaotic system

It can be seen from Fig. 2 that all the characteristic roots in the black area satisfy $q\pi/2<|\arg(\lambda_i)|$, which means that system is stable. In the white area, all the characteristic roots

satisfy $|\arg(\lambda_i)|\leq q\pi/2$, and the system is unstable at this time.

For q=1, a system with integer order is obtained. If only consider the case of $q_1=q_2=q_3=q$, that is, all variables in the system have the same order, then the following theorem can be used to analyze the system state [16].

Theorem 2: Assume that the unstable characteristic root of the rolling saddle point is $\lambda_{2.3}=r_{2.3}\pm j\omega_{2.3}$. If and only if the characteristic root $\lambda_{2.3}$ is located in the unstable region. This is a chaotic system. The equal order in the fractional-order system satisfies $q > (\pi/2)a\tan(|\omega_{2.3}|/r_{2.3})$.

4.2 Phase diagram of the system

Set $[x_0, y_0, z_0]$ = [0.1, 0, 0], d=1/3, c=1, β=1.5, α=0.6, h=0.01, and q=0.545. Fig. 3 plots the phase diagram of the system. The L_1=0.346, L_2=0, L_3=-8.166. We can see that the largest Lyapunov exponent is greatly improved compared to the integer order state.

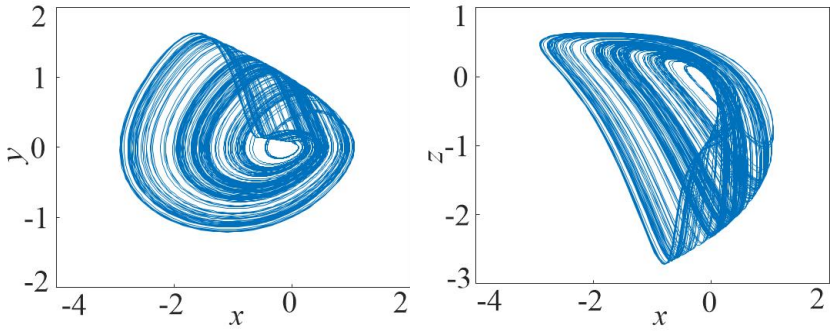

(a) (b)

Fig.3 Phase diagram of the system (a) x-y plane (b) x-z plane

4.3 LEs and bifurcation diagram of chaotic system

Taking the initial value is [0.1, 0, 0] and c=1, d=1/3, α=0.6, β=1.5, h=0.01. When $q\in$[0.3, 1], Fig. 4 depicts the LEs and bifurcation diagrams of the chaotic system.

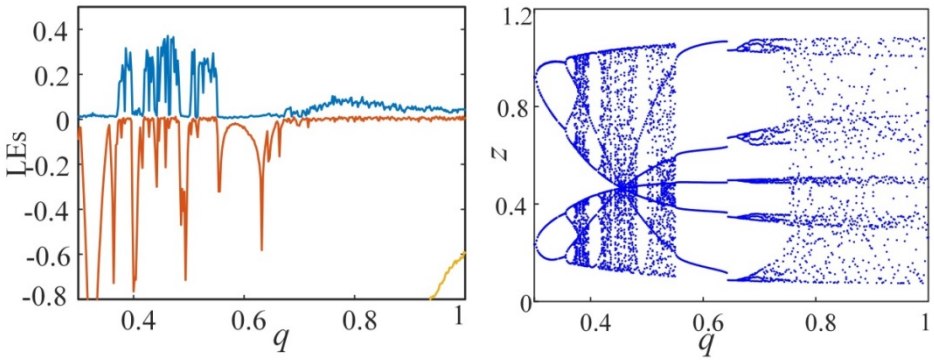

(a) (b)

Fig.4 LEs and bifurcation diagram of q (a) LEs (b) Bifurcation diagram

The analysis found that the performance of the fractional-order system has been greatly improved. In addition, the smallest order of chaos in this system is q=0.38×3=1.14. Table 1 lists the state of the system under different q.

Table 1. Dynamic characteristics when the order q changes

q	Dynamical characteristics	q	Dynamical characteristics
0~0.3	divergence	0.45~0.48	chaotic state
0.3~0.34	4 cycle	0.49~0.5	7 cycle
0.35~0.37	8 cycle	0.51~0.55	chaotic state
0.38~0.39	chaotic state	0.56~0.57	5 cycle
0.4~0.41	6 cycle	0.68~0.69	chaotic state
0.42~0.43	chaotic state	0.7	15 cycle
0.44	8 cycle	0.71~1	chaotic state

When q is less than 0.3, the system is divergent. When q is between 0.3 and 1, the system has typical chaotic attractors and many different periodic states.

Let q=0.545 and fix other parameters unchanged. By changing the parameter β, the LEs and bifurcation diagram are plotted in Fig. 5. From Fig. 5, when β takes different values, the LEs obtained correspond to the state of the bifurcation diagram.

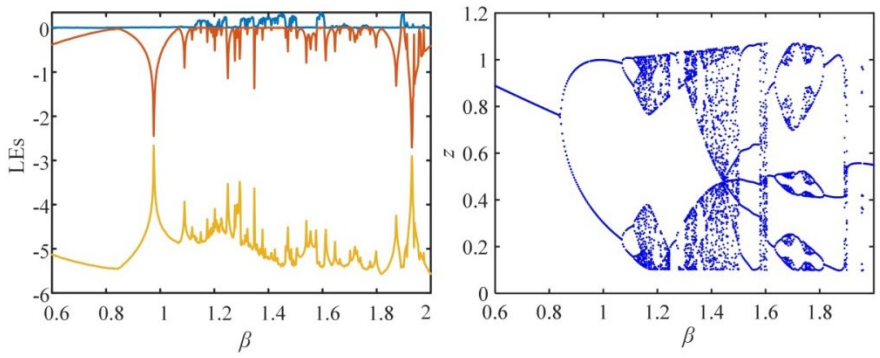

(a) (b)

Fig.5 LEs and bifurcation diagram of β (a) LEs (b) Bifurcation diagram

Table 2 shows the state of the system when β changes. It can be seen from Table 2 that when $\beta \in [0.6, 2]$, the system has a classic chaotic attractor and seven different periodic states, and typical periodic doubling branches and anti-periodic branches appear in the process.

Table 2. Dynamic characteristics when the parameter β changes

β	Dynamical behaviors	β	Dynamical behaviors
0.6~0.9	1 cycle	1.45~1.47	6 cycle
0.91~1.14	2 cycle	1.48	chaotic attractor
1.15~1.28	4 cycle	1.49	8 cycle
1.29~1.32	2 cycle	1.5~1.56	chaotic attractor
1.32~1.33	4 cycle	1.57~1.61	5 cycle
1.33~1.36	8 cycle	1.62~1.67	chaotic attractor
1.36	chaotic attractor	1.68~1.71	3 cycle
1.37	8 cycle	1.72~1.82	6 cycle
1.38	chaotic attractor	1.83~1.88	3 cycle
1.39~1.42	4 cycle	1.89~1.97	chaotic attractor
1.43~1.44	chaotic attractor	1.98~2	Limit cycle

4.4 Complexity of chaotic systems

Complexity is a significant indicator for measuring chaotic pseudo-random sequences. Random performance is better for sequences with high complexity. When applying chaotic sequences to these fields, it is necessary to select sequences with higher randomness and stronger complexity. At present, the commonly used methods for dynamic analysis of chaotic systems include LEs and bifurcation diagram. The two methods can qualitatively evaluate the system's feature, but cannot quantitatively reflect the complexity and randomness of the chaotic sequence. Therefore, spectral entropy (SE) and C_0 complexity are selected to evaluate the randomness of the chaotic system, so that chaotic sequences with higher complexity are selected when the system is applied to chaotic image encryption.

Set c=1, d=1/3, α=0.6, step h=0.01, and [x_0, y_0, z_0] = [0.1, 0, 0]. Based on complexity algorithm, when q and β change at the same time, the complexity of the chaotic system is displayed in Fig. 6.

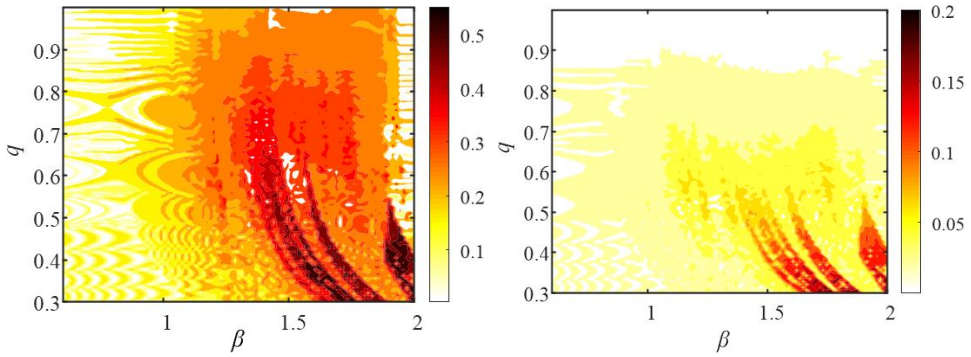

(a) (b)

Fig.6 Complexity of the chaotic system when q and β change simultaneously (a) SE complexity (b) C_0 complexity

From Fig. 6, the darker colors represent higher levels of complexity. From the Fig.6, when SE is 0.55 the system is the most complex, in this case order q=0.41, the parameter β=1.9, the maximum C_0 complexity is 0.21, the order q=0.33, and the parameter β=1.78. The two complexity changes in Fig. 6 (a) and (b) have the same trend, but the specific values are quite different. Because the spectral entropy (SE) complexity is calculated according to the energy distribution of the system; and the C_0 complexity is Remove the regular part in the sequence, and then analyze and calculate the irregular part; the two algorithms are different, which leads to deviations in specific values. However, both of these two complexity algorithms can express the dynamics of the system and the process of entering chaos, and the trends of the two are consistent. In summary, when β=1.94, 0.4<q<0.5, the complexity and randomness of the system are better. Therefore, when we apply the system, the chaotic sequence in this area should be selected as much as possible.

4.5 Randomness of chaotic system

One of the methods to effectively check the sequence's close to random sequence is the NIST test, which contains 15 performance indicators to check the randomness of the chaotic sequence. Generally speaking, the result meets two criteria, that is, the sequence passed the NIST test.

The first criterion is that the test result obtains the P value, which intuitively reflects whether the sequence is uniformly distributed, and is calculated according to the following

formula:

$$\begin{cases} \chi^2 = \sum_{i=1}^{10} \frac{(F_i - 0.1m)^2}{0.1m} \\ P - value = \text{igmac}(4.5, \frac{\chi^2}{2}) \end{cases}, \tag{24}$$

here F_i is the number of P-value, m represents how many groups. If the P-value>0.01, the randomness of the reconstructed fractional chaotic system has passed the randomness test and has good performance.

Another criterion is the pass rate of passing the test, that is, the proportion of the sequence that passes the test in the entire sequence. We believe that when the following formula is

$$1 - \alpha \pm \sqrt{\frac{\alpha(1-\alpha)}{m}}, \tag{25}$$

where $m \geqslant 1000$ and the value of α is 0.01. The chaotic sequence detection report is compared with the reference [26] in Table 3.

Table 3. NIST test

Test items	Ours		Ref [26]	
	P-value	Pass rate	*P*-value	Pass rate
Frequency	0.275709	0.98	0.867692	0.99
Block Frequency	0.224821	0.98	0.77918	1
Cumulative Sums	0.275709	0.98	0.739918	0.99
Runs	0.249284	0.99	0.779188	0.98
Longest Run	0.350485	0.99	0.055361	1
Rank	0.055361	0.98	0.474986	0.99
FFT	0.851383	1	0.062821	1
Non Overlapping Template	0.162606	0.99	0.071177	0.99
Overlapping Template	0.637119	0.98	0.013569	0.99
Universal	0.262249	1	0.108791	0.99
Approximate Entropy	0.304126	0.99	0.759756	1
Random Excursions	0.249284	0.98	0.249284	0.98
Random Excursions Variant	0.062821	0.98	0.025193	0.98
Serial	0.445368	0.99	0.137282	0.98
Linear Complexity	0.071177	0.99	0.227821	0.97

4.6 DSP realization of chaotic system

Use DSP platform to achieve the chaotic system. The hardware implementation platform is displayed in Fig. 7. Among them, the DSP chip with model TMS320F28335 is used, and the D/A converter is DAC8552, and the oscilloscope is UTD7102H.

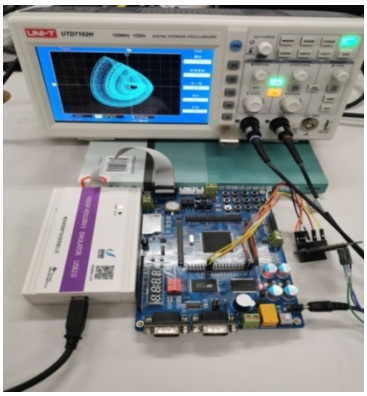

Fig. 7 DSP hardware platform

Setting parameters are shown in section 4.2, and the phase diagram implemented by the DSP platform is plotted in Fig. 8(a)-(c), it is consistent with the computer simulation.

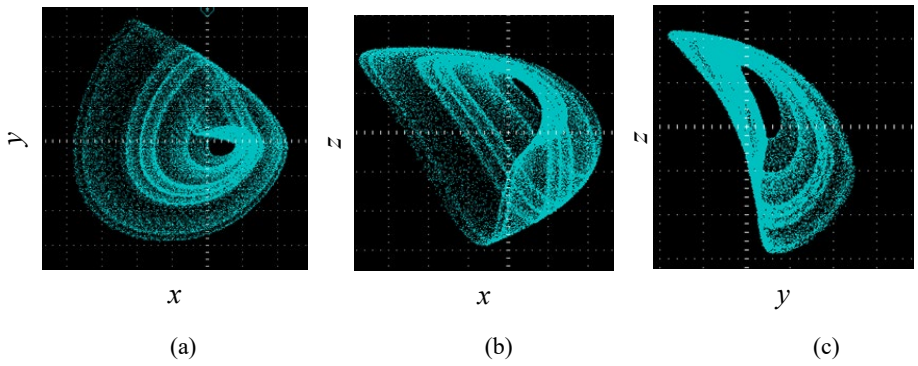

Fig. 8 Phase diagram (a) *x*-*y* plane (b) *x*-*z* plane (c) *y*-*z* plane

5. Conclusion

According to the definition of fractional differential and the memristive chaotic circuit, we construct the fractional form, and the solution of the chaotic system is calculated using ADM algorithm. On this basis, the system's dynamic features are studied using phase diagram, LEs, bifurcation diagram, and complexity. The analysis of dynamic characteristics shows that the application of ADM decomposition algorithm can effectively solve the fractional-order chaotic system, and the proposed chaotic system has complex performance. When the parameter β=1.94 and the order $q \in (0.4,0.5)$, the randomness and complexity of the system are the best. Under this condition, the chaotic sequence obtained is more suitable for chaotic applications. The process of solving the fractional order chaotic system is realized on the DSP

platform, and the approximate attractor is obtained on the oscilloscope. The conclusions obtained from this research provide great help for the application of memristive chaotic circuits based on fractional order.

Reference

[1] L. Chua, "Memristor-The missing circuit element," IEEE Transactions on Circuit Theory, vol. 18, no. 5, pp. 507-519, 1971.

[2] L. O. Chua and K. Sung Mo, "Memristive devices and systems," Proceedings of the IEEE, vol. 64, no. 2, pp. 209-223, 1976.

[3] L. O. Chua, "The Fourth Element," Proceedings of the IEEE, vol. 100, no. 6, pp. p.1920-1927, 2012.

[4] F. Corinto, A. Ascoli, and M. Gilli, "Nonlinear Dynamics of Memristor Oscillators," IEEE Transactions on Circuits & Systems I Regular Papers, vol. 58, no. 6, pp. 1323-1336, 2011.

[5] L. Teng, H. H. C. Iu, X. Wang, and X. Wang, "Chaotic behavior in fractional-order memristor-based simplest chaotic circuit using fourth degree polynomial," Nonlinear Dynamics, vol. 77, no. 1-2, pp. 231-241, 2014.

[6] B. C. Bao, Z. Liu, and J. P. Xu, "Steady periodic memristor oscillator with transient chaotic behaviours," Electronics Letters, vol. 46, no. 3, pp. 237-238, 2010.

[7] B. Zhang and F. Deng, "Double-compound synchronization of six memristor-based Lorenz systems," Nonlinear Dynamics, vol. 77, no. 4, pp. 1519-1530, 2014.

[8] X. Ye, J. Mou, C. Luo, F. Yang, and Y. Cao, "Complexity Analysis of a Mixed Memristive Chaotic Circuit," Complexity, vol. 2018, pp. 1-9, 2018.

[9] X. Ye, J. Mou, C. Luo, and Z. Wang, "Dynamics analysis of Wien-bridge hyperchaotic memristive circuit system," Nonlinear Dynamics, 2018.

[10] F. Yu, L. Liu, H. Shen, Z. Zhang, and Q. Wan, "Multistability Analysis, Coexisting Multiple Attractors, and FPGA Implementation of Yu–Wang Four-Wing Chaotic System," Mathematical Problems in Engineering, vol. 2020, pp. 1-16, 2020.

[11] F. Yu et al., "Dynamic Analysis, Circuit Design, and Synchronization of a Novel 6D Memristive Four-Wing Hyperchaotic System with Multiple Coexisting Attractors," Complexity, vol. 2020, 2020.

[12] M. Jun, S. Kehui, W. Huihai, and R. Jingya, "Characteristic Analysis of Fractional-Order 4D Hyperchaotic Memristive Circuit," Mathematical Problems in Engineering, vol. 2017, pp. 1-13, 2017.

[13] Y. Xu, K. Sun, S. He, and L. Zhang, "Dynamics of a fractional-order simplified unified system based on the Adomian decomposition method," European Physical Journal Plus, vol. 131, no. 6, pp. 1-12, 2016.

[14] S. He, K. Sun, X. Mei, B. Yan, and S. Xu, "Numerical analysis of a fractional-order chaotic system

based on conformable fractional-order derivative," European Physical Journal Plus, vol. 132, no. 1, p. 36, 2017.

[15] L. Zhang, K. Sun, S. He, H. Wang, and Y. Xu, "Solution and dynamics of a fractional-order 5-D hyperchaotic system with four wings," European Physical Journal Plus, vol. 132, no. 1, p. 31, 2017.

[16] I. Petras, "Fractional-Order Memristor-Based Chua's Circuit," IEEE Transactions on Circuits & Systems II Express Briefs, vol. 57, no. 12, pp. 975-979, 2010.

[17] Ivopetr, "CHAOS IN FRACTIONAL-ORDER POPULATION MODEL," International Journal of Bifurcation & Chaos, vol. 22, no. 4, 2012.

[18] T. T. Hartley, C. F. Lorenzo, and H. K. Qammer, "Chaos in a fractional order Chua's system," Circuits & Systems I Fundamental Theory & Applications IEEE Transactions on, vol. 42, no. 8, pp. 485-490, 1995.

[19] D. Cafagna and G. Grassi, "AN EFFECTIVE METHOD FOR DETECTING CHAOS IN FRACTIONAL-ORDER SYSTEMS," International Journal of Bifurcation & Chaos, vol. 20, no. 03, pp. 1002595-, 2010.

[20] H. Y. Jia, Z. Q. Chen, and G. Y. Qi, "Chaotic Characteristics Analysis and Circuit Implementation for a Fractional-Order System," IEEE Transactions on Circuits & Systems I Regular Papers, vol. 61, no. 3, pp. 845-853, 2017.

[21] W. Gu, Y. Yu, and W. Hu, "Artificial Bee Colony Algorithm-based Parameter Estimation of Fractional-order Chaotic System with Time Delay," IEEE/CAA Journal of Automatica Sinica, vol. 4, no. 1, pp. 107-113, 2017.

[22] M. S. Tavazoei and M. Haeri, "Unreliability of frequency-domain approximation in recognising chaos in fractional-order systems," Iet Signal Processing, vol. 1, no. 4, pp. 171-181, 2007.

[23] M. S. Tavazoei and M. Haeri, "Limitations of frequency domain approximation for detecting chaos in fractional order systems," Nonlinear Analysis Theory Methods & Applications, vol. 69, no. 4, pp. 1299-1320, 2008.

[24] S. B. He, K. H. Sun, and H. H. Wang, "Solution of the fractional-order chaotic system based on Adomian decomposition algorithm and its complexity analysis," Acta Physica Sinica, vol. 63, no. 3, pp. 030502-72, 2014.

[25] D. Cafagna and G. Grassi, "BIFURCATION AND CHAOS IN THE FRACTIONAL-ORDER CHEN SYSTEM VIA A TIME-DOMAIN APPROACH," International Journal of Bifurcation & Chaos, vol. 18, no. 07, pp. 1845-1863, 2008.

[26] F. Yang, J. Mou, K. Sun, Y. Cao, and J. Jin, "Color Image Compression-Encryption Algorithm Based on Fractional-Order Memristor Chaotic Circuit," IEEE Access, vol. 7, pp. 58751-58763, 2019.